

Coupled Effects in Quantum Dot Nanostructures with Nonlinear Strain and Bridging Modelling Scales

Roderick Melnik and Roy Mahapatra

*Mathematical Modelling & Computational Sciences,
Wilfrid Laurier University, Waterloo Campus,
75 University Avenue West, Waterloo, ON, Canada N2L 3C5*

Abstract

We demonstrate that the conventional application of linear models to the analysis of optoelectromechanical properties of nanostructures in bandstructure engineering could be inadequate. Such linear models are usually derived from the traditional bottom-up approach applied to the analysis of nanostructure properties. At the same time, in the hierarchy of mathematical models for semiconductor device modelling constructed on the basis of the top-down approach, we deal predominantly with models where nonlinearity is essential. In this contribution, we analyze these two fundamental approaches in bridging the scales in mathematical models for the description of optoelectromechanical properties of nanostructures. The focus of the present paper is on a model based on the coupled Schrodinger-Poisson system where we account consistently for the piezoelectric effect and analyze the influence of different nonlinear terms in strain components. The examples given in this paper show that the piezoelectric effect contributions are essential and have to be accounted for with fully coupled models. While in structural applications of piezoelectric materials at larger scales, the minimization of the full electromechanical energy is now a routine in many engineering applications, in bandstructure engineering conventional approaches are still based on linear models with minimization of uncoupled, purely elastic energy functionals with respect to displacements. Generalizations of the existing models for bandstructure calculations are presented in this paper in the context of coupled effects.

Key words: Coupled effects, fluid-dynamics approximations, nonlinear strain, nanostructures, piezoelectric materials.

1 Introduction

In low-dimensional semiconductor nanostructures (LDSN) the motion of electrons can be confined spatially, from one, two, and even three spatial directions. In the latter case, such nanostructures are known as quantum dots and often termed by physicists as 0-dimensional structures, reflecting the fact that the motion of carriers is constrained from all three spatial directions. These structures have been receiving an increasing interest due to new technological advances and fascinating applications they offer. Indeed, they can be used as biological tags in cell biology and biomedicine, be used in constructing quantum bits for quantum computing, and be applied in a wide range of more traditional structure- and device-like applications, including photodecoders, laser-based emitters, etc.

While in many such applications the focus is on optical properties of future devices, it is important to remember that the formation of LDSNs, and in particular quantum dots, is a competition between the surface energy in the structure and strain energy. Hence, mechanical properties are essential in designing quantum-dot-based devices and structures. Further, many quantum dot structures have a well pronounced piezoelectric effect which does contribute to their overall properties in a non-trivial manner. These coupled electromechanical effects will become increasingly important for the current and future applications of such nanostructures. In designing stable strained nanostructures, computational modelling provides a major tool for predicting their optoelectromechanical properties.

During the last decade, the attention of the science and engineering community to the influence of strain effects on quantum mechanical properties of LDSNs has been growing rapidly [1,2,3,4,5]. A majority of the published works were focusing on strain effects only, without taking into account electromechanical interactions due to the piezoelectric effect. Those authors who did account for the piezoeffect based their considerations on the minimization of uncoupled, purely elastic energy functionals with respect to displacements. Under this approach, the Maxwell equation for piezoelectric solids and the equations of elasticity were effectively solved in either uncoupled or semicoupled manner. Pan with his collaborators [6,7] were the first who have attracted the attention of the bandstructure engineering community to the importance of coupled effects. Based on his semi-analytical Green's function approach applied to an idealized half-space structure [6], he demonstrated that only the fully coupled model can lend a reliable prediction. Further, based on a combination of analytical (for the 1D case) and numerical (for the 2D case) techniques, the idea was generalized to the device level [7], but no details of the numerical procedure were given. All the above studies were based on the linear theory only. Furthermore, the nature of the analyzed problem allowed a number of

simplifications, including those related to the wetting layer. The inclusion of the wetting layer in a consistent manner not only increase the computational complexity of the problem in several times due to different spatial scales, but may also require the formulation of non-trivial boundary conditions [8].

In this paper, we base our consideration on the coupled Schrodinger-Poisson model where we account consistently for the piezoelectric effect and analyze the influence of different nonlinear terms in strain components. We structure the paper as follows. In Section 2, we analyze two fundamental approaches in bridging the scales in mathematical models for the description of optoelectromechanical properties of nanostructures. In Section 3, we provide the core model for the description of coupled electromechanical interactions in piezoelectric semiconductor solids. The model is exemplified for hexagonal (WZ) and cubic (ZB) materials used in our computational experiments. In Section 4, we give details of the model for bandstructure calculations, focusing on the $\mathbf{k} \cdot \mathbf{p}$ approximation as a convenient framework for incorporating strain and piezoelectric effects. A general procedure for modelling quantum dot nanostructures, based on the variational formulation of the problem, is outlined in Section 5. In Section 6 we provide details of numerical experiments demonstrating the influence of the piezoelectric effect and analyzing contributions of nonlinear terms in strain components. Conclusions are given in Section 7.

2 Waves propagation in anisotropic media: applying experience from solid and fluid mechanics to bandstructure engineering

Waves propagation in anisotropic media has always been a topic in the heart of scientific inquiries and a source of new ideas for engineers. This topic is of immense practical importance in the context of both solid and fluid mechanics. Purely elastic waves in shells and other structures have been studied in the context of fluid-solid interactions at least since the late 1950ies, providing many meaningful examples where coupling effects become essential. Around the same time, an increasing interest to coupled problems was also generated by the analysis of dynamic thermal stresses in structures, in particular by the famous Danilovskaya problem, first formulated in 1950. Since then, coupled effects, in particular in anisotropic materials, have continued to fuel interest to their studies due to both, theoretical challenges and an increasing range of practical applications.

In what follows, we will focus on the coupling between electric and mechanical fields in low-dimensional semiconductor nanostructures. The core of the mathematical models dealing with this sort of coupling contains the equations for coupled electromechanical motion of piezoelectric solids. The experience accumulated in mechanics of solids in solving such equations becomes now

invaluable in the area known as bandstructure engineering and in the modelling semiconductor quantum structures in general. At the same time, the experience accumulated in fluid dynamics applications is equally important in this area. Indeed, the hydrodynamic approach in the analysis of semiconductor devices, superlattices, and other semiconductor structures has been an important tool in semiconductor modelling for a number of years. Fluid-dynamics-like hydrodynamic approximations have been widely utilized in this area and more recently several their extensions have been proposed to account for quantum effects. The importance of such semiconductor systems as quantum wells, wires, dots, and superlattices [9] will continue to grow in nanoscale electronics, photonics, and bioengineering. New technological advances in applications of these structures require to have a fresh look at their modelling aspects, in particular in the context of their optoelectromechanical properties. While strain effects are fundamental to such properties, in the bandstructure engineering literature their influence is still typically analyzed with simplified linear models based on the minimization of uncoupled, purely elastic energy functionals with respect to displacements. The applicability of such models is limited as coupled effects related, e.g., to built-in spontaneous and piezoelectric polarization become essential. New models accounting for these effects need to be developed.

The modelling experience accumulated in both mechanics of solids and fluid mechanics can help in achieving this task. To get started, note that in semiconductor systems we are dealing with, both classical and quantum effects are interlinked, and the analysis of such systems and the choice of modelling tools depend critically on the spatio-temporal scales required for specific applications. We can start constructing a model for the analysis of such systems from the fundamental quantum level by specifying the Hamiltonian of the system within the Schrodinger framework. However, then we should incorporate additional effects, pronounced at larger scales, such as piezoelectric, into the obtained approximate model. This is *the bottom-up approach* to modelling semiconductors, applied actively today for the analysis of nanostructures. Alternatively, we can attempt to carry out some physics-based averaging right from the beginning, applying *the top-down approach* to modelling semiconductors. A good example, clarifying conceptually the applicability and limitations of these approaches, can be provided by considering models for superlattices. Based on the underlying physical assumptions, there are two major classes of such structures, classical and quantum. These structures have additional periodicity on a scale larger than atomic. The idea of creating quantum superlattices is due to L. Keldysh (1962). Experimentalists reported the creation of such objects about a decade later (L. Esaki, 1970; Zh. Alferov et al, 1971). It has been the domain of solid state physics where tools of solid mechanics are essential and well established. On the other hand, the idea of creating classical semiconductor superlattices was originated from a fluid mechanics analogy. It is well known (e.g., [10] and references therein) that a fluid under gravity can

reach its equilibrium if its temperature depends on the height only. If the temperature gradient, directed down, exceeds certain critical value, we observe a free convection of the fluid. If we assume that this process takes place between two infinitely long horizontal planes heated to different temperatures (temperature of the lower plane is higher), under a sufficiently high temperature gradient the fluid becomes unstable and we observe stationary convective motion. Due to the underlying assumptions, in the horizontal plane the motion is expected to be periodic. Based on this hydrodynamic analogy, a similar idea was proposed in early 1970ies in the context of carrier motion in semiconductors, where the role of gravitational field could be played by the electric field with heating produced by, e.g., light ([10] and references therein). The analogy between wave phenomena in classical superlattices and the behaviour of wave functions of an electron moving in a periodic potential field of a quantum superlattice can be exploited when developing a hierarchy of models for the analysis of semiconductor structures. In both cases, we have an additional periodicity of the structure. However, the difference between these two cases lies in the fact that while for classical superlattices such an additional periodicity leads to the quantization of wave energy, in quantum superlattices it leads to the quantization of carrier energy. If the period of the potential field exceeds the length of free carrier runs, so that on this specific spatio-temporal scale carriers will not be affected by the action of the additional periodic field, semiconductor superlattices behave like classical structures. In the latter case, many (fluid-mechanics analogy based) techniques developed for semiconductor device modelling at sub-micron scales can often be applied. The study of quantum superlattices requires more fundamental approaches to account for atomic scales.

Note that already at the classical level we have to construct a multiscale hierarchy of the models. Indeed, the standard drift-diffusion approximation may not be an appropriate modelling tool even for classical superlattices, while hydrodynamic and kinetic models provide quite useful tools for the analysis of such structures. Based on relaxation time approximations, a classification of the hierarchy of mathematical models for these structures was discussed in [11,21]. At the top of this hierarchy is the Liouville equation framework which leads to substantial difficulties in practical realization of this approach. Hence, most practical approaches stem from the kinetic-type models such as the semi-classical Boltzmann equation. In these models, scattering of carriers on each other is not essential. However, the scattering of carriers on imperfections of the lattice plays the dominant role. Hence, charge carriers under this approach cannot be considered as an independent thermodynamical system. Based on the moment methodology or the Hilbert expansion method, a range of macroscopic models can be derived, among which hydrodynamic-type models play a prominent role. In such models the electron-hole "plasma" can be considered as an almost independent thermodynamical system that only weakly interacts with the crystal lattice. This group of models as well

as quasi-hydrodynamic models can account for non-equilibrium and non-local behaviour of semiconductor carrier "plasma". Further details of the developed computational techniques for such models can be found in [21,11,12]. We note that the equations we deal with in such situations are similar to, but differ from, the hydrodynamic equations of fluid mechanics. They consist of the Poisson equation, equations of continuity (for carrier concentrations) and energy transfer. Furthermore, re-distributions of charge carriers lead to an additional field, a phenomenon absent in the fluid mechanics. Attempts to apply these types of models to other semiconductor structures and devices at smaller scales have led recently to the development of extended hydrodynamic models that should incorporate quantum corrections [13]. The important observation is that all the models we have discussed above within the top-down approach are intrinsically nonlinear.

At the other end of the spectrum of model hierarchy are the models developed with the bottom-up approach. Surprisingly, up to date the majority of research efforts in this area has been concentrated on linear models. In what follows, we focus on the analysis of quantum dot structures and show that the conventional approaches to the analysis of these structures based on linear models need to be augmented to account for coupled nonlinear effects.

3 Coupled electromechanical interactions in quantum dot nanostructures

Mechanical effects profoundly influence electronic and optical properties of the nanostructures. Two points should be mentioned in this context. Firstly, we note that the key to intrinsic properties of quantum dot structures lies with strain effects arising from lattice mismatch. Following [14], where the authors started their reasoning from the total Helmholtz free energy function, we assume that there is the local equilibrium value of the lattice constant. Hence, the lattice mismatch can be incorporated in the models for bandstructure calculations by defining the strain associated with it as a mismatch between two material layers

$$\varepsilon_m = (a^0 - a(\mathbf{r}))/a^0, \quad (1)$$

and by accounting for it in the strain-displacement relationships. In (1), $a(\mathbf{r})$ and a^0 are lattice constants of two different material layers, respectively, while \mathbf{r} is the position vector responsible for tracking the interface. This aspect of mechanical effect contributions has been actively incorporated into the theory of bandstructure calculations since early 1970s, starting from fundamental works by Pikus, Bir, Rasba, Sheka and many others [15]. Secondly, semicon-

ductors are piezoelectric materials and the piezoelectric effect contributions to the overall properties cannot be ignored in bandstructure engineering, neither for hexagonal (wurtzite) structures (often due to the principle strain components) nor for cubic (zinc-blende) structures (often due to the shear strain components). Piezoelectrics represent anisotropic media and wave interactions in such media have been a topic of immense practical importance. While purely elastic waves in structures have been studied intensively for many decades, the study of coupled electromechanical interactions in anisotropic materials is of more recent origin. One reason for that lies with the fact that dealing with problems of coupled electroelasticity usually requires the development and implementation of effective numerical techniques [16]. Hence, the experience that has been accumulated in solving problems of coupled electroelasticity for piezoelectric structures becomes invaluable in the area of bandstructure engineering and modelling semiconductor quantum structures. As in the other areas where modelling piezoelectric solids is an essential component, we consider the following general model (e.g., [16]), describing coupled electromechanical interactions in the Cartesian system of coordinates $\mathbf{x} = (x_1, x_2, x_3)^T$:

$$\rho \frac{\partial^2 \mathbf{u}}{\partial t^2} = \nabla \cdot \boldsymbol{\sigma} + \mathbf{F}, \quad \text{div} \mathbf{D} = \mathbf{G}, \quad \mathbf{E} = -\nabla \varphi, \quad (2)$$

where $\mathbf{u} = (u_1, u_2, u_3)^T$ is the displacement vector, $\boldsymbol{\sigma} = (\sigma_{ij})$ is the stress, ρ is the density of the piezoelectric material, \mathbf{F} and \mathbf{G} are body and electric forces on the piezoelectric, if any, \mathbf{E} and \mathbf{D} are the electric field and electric displacement, and φ is the electrostatic potential. The conventional procedure applied in modelling LDSNs is based on the minimization of the purely elastic functionals (e.g., [4]), rather than on the solution of the fully coupled problem. The effect of coupling has been analyzed rigorously in a general setting in [18,19,16] (see also references therein), while in the context of nanostructure modelling it has recently been demonstrated that such an effect could be quite substantial [6,7]. The core component of our model for analyzing the properties of quantum dot nanostructures will be the equilibrium equations of the coupled theory of electroelasticity which are simplified in this case to

$$\partial \sigma_{ij} / \partial x_j = 0, \quad \text{div} \mathbf{D} = 0, \quad (3)$$

where the coordinate subindices in the Timoshenko-Karman notions are obtained by changing $1 \rightarrow x$, $2 \rightarrow y$, $z \rightarrow 3$ in the tensorial representation above. The type of coupling between the mechanical and electric fields is determined by the type of the crystallographic symmetry of the material. In particular, for the WZ semiconductors we have

$$\sigma_{xx} = c_{11}\varepsilon_{xx} + c_{12}\varepsilon_{yy} + c_{13}\varepsilon_{zz} - e_{13}E_z, \quad \sigma_{xy} = (c_{11} - c_{12})\varepsilon_{xy}/2,$$

$$\begin{aligned}
\sigma_{yy} &= c_{12}\varepsilon_{xx} + c_{11}\varepsilon_{yy} + c_{13}\varepsilon_{zz} - e_{31}E_z, & \sigma_{yz} &= c_{44}\varepsilon_{yz} - e_{15}E_y, \\
\sigma_{zz} &= c_{13}(\varepsilon_{xx} + \varepsilon_{yy}) + c_{33}\varepsilon_{zz} - e_{33}E_z, & \sigma_{zx} &= c_{44}\varepsilon_{zx} - e_{15}E_x, \\
D_x &= e_{15}\varepsilon_{zx} + \epsilon_{11}E_x, & D_y &= e_{15}\varepsilon_{yz} + \epsilon_{11}E_y, \\
D_z &= e_{31}(\varepsilon_{xx} + \varepsilon_{yy}) + e_{33}\varepsilon_{zz} + \epsilon_{33}E_z + P_{\text{sp}}, & & (4)
\end{aligned}$$

where e_{ij} and ϵ_{ii} are piezoelectric and dielectric coefficients; P_{sp} is the spontaneous polarization. While for the WZ materials the built-in spontaneous polarization and the principal components of strain are main contributors to the piezoelectric effect contributions, in ZB materials it is the shear strain components that may contribute noticeably to the overall properties. For such materials we have the following constitutive relationships that couple (3):

$$\begin{aligned}
\sigma_{xx} &= c_{11}\varepsilon_{xx} + c_{12}\varepsilon_{yy} + c_{12}\varepsilon_{zz}, & \sigma_{yy} &= c_{12}\varepsilon_{xx} + c_{11}\varepsilon_{yy} + c_{12}\varepsilon_{zz}, \\
\sigma_{zz} &= c_{12}\varepsilon_{xx} + c_{12}\varepsilon_{yy} + c_{11}\varepsilon_{zz}, & \sigma_{yz} &= 4c_{44}\varepsilon_{yz} - e_{14}E_x, \\
\sigma_{zx} &= 4c_{44}\varepsilon_{zx} - e_{14}E_y, & \sigma_{xy} &= 4c_{44}\varepsilon_{xy} - e_{14}E_z, \\
D_x &= e_{14}\varepsilon_{yz} + \epsilon_{11}E_x, & D_y &= e_{14}\varepsilon_{zx} + \epsilon_{22}E_y, & D_z &= e_{14}\varepsilon_{xy} + \epsilon_{33}E_z. & (5)
\end{aligned}$$

The issue of coupling via boundary conditions remains largely untouched in the area of modelling piezoelectric semiconductor nanostructures, in particular when the wetting layer is taken into account. The formulation of correct boundary conditions in the latter case was discussed in [8]. Recall that the model we presented in [8] accounted for electron states with arbitrary kinetic energies in the wetting layer. Effectively, the model we derived for the quantum dot structure with wetting layer allowed us to demonstrate several important observations. In particular, electron states that correspond to a single quantum dot structure with wetting layer will asymptotically approach one of the two limiting situations: either "pure" quantum well states far away from the quantum dot region or zero in the case of a "pure" quantum dot state. This observation must be used, as explained in [8], for the formulation of general boundary conditions for the combined quantum-dot/wetting-layer structure.

The resulting problem we deal with in this paper is a boundary value problem that is solved with respect to (u_1, u_2, u_3, φ) . From a mechanics point of view, the model is derived from a variational principle applied to the total potential energy which includes both deformational energy and piezoelectric field functionals as described in [19,16]. Variational difference schemes developed in [16], as well as the finite element formulation developed for computations in this paper, follow from such a variational representation. Finite element methodologies have been previously applied to bandstructure analysis in [3,17,20]. However, in these papers the contribution of piezoelectric effect was not ac-

counted for. All works in this area we are aware of are based so far on the linear theory of elasticity.

Taking into account piezoelectric effect contributions, in the subsequent sections we will compare the results for bandstructure calculations and the prediction of optoelectromechanical properties of nanostructures that are obtained with linear and nonlinear strain models.

4 Bridging the scales to the quantum effect level and exploiting the analogy with coupled models of structural mechanics

Already today, quantum effects play an important role in many optoelectronic devices and structures. This trend will persist into the future as device miniaturization continues. Therefore, ideally the full bandstructure transport description is required. However, at present it is not possible in practice, in particular at the device/structure level. The reason is simple: transport should be computed with a many-particle Hamiltonian for the carriers and the atomic structures of the device/structure material. This is a task of enormous computational complexity, not feasible to complete today. Hence, some simplifications need to be made.

One approach is to account for quantum mechanical (and statistical) effects via the Wigner-Boltzmann model. Although such a model also involves substantial computational difficulties, it allows us to construct a hierarchy of the macroscopic models in a way similar to those involving fluid dynamics problems and semiconductor device theory where the continuity (fluid-like) analogy is used for the model classification (e.g., [21] and references therein). At present, most of the quantum corrected macroscopic models are in their infancy as they are usually not able to adequately include interactions between the electrons and other particles. New efforts in this direction are currently being undertaken by a number of authors (e.g., [22]). Since the problem we are addressing is a *multiscale* problem, a natural way to approach its solution in the above framework could be to apply a domain decomposition technique. For example, one can use the quantum mechanical approach in the regions where quantum mechanical effects are dominant and use continuum-like (e.g., hydrodynamic) models in other regions. However, the issue of coupling such models, e.g., via an interface condition of a typical domain decomposition methodology or by using other techniques, is far from trivial and remains largely open.

In this paper we follow another route. While the application of ab initio and atomistic methodologies are inheritably problematic from a computational complexity point of view, we resort to averaging procedures over atomic scales. This can be achieved by a variety of procedures, including various empirical

tight-binding, pseudopotential, and $\mathbf{k} \cdot \mathbf{p}$ approximations. In what follows, we focus on the latter approximation as a tool for averaging over atomic scales. The procedure stems from the original work by Luttinger-Kohn and is based on the effective mass approximation and the subsequent development of the $\mathbf{k} \cdot \mathbf{p}$ theory. As with any model, the one we develop here relies on a set of assumptions some of which may not be always fulfilled. For example, a typical assumption of the $\mathbf{k} \cdot \mathbf{p}$ theory that potentials change slowly on the length scale of the lattice constant could be questionable for Metal-Oxide-Semiconductor Field-Effect (MOSFE) devices, e.g. Nevertheless, in bandstructure calculations of LDSNs, the theory provides a remarkably flexible tool. Furthermore, while we do not address this issue in detail in this paper, it is worthwhile mentioning that a recent refined approximation of the Luttinger-Kohn Hamiltonian, known as the Burt-Foreman correction, has been developed and tested (see examples and further details in [23]). This correction allows us to put the effective mass theory formalism related to the behaviour of the envelope functions across interfaces on a much more rigorous mathematical foundation.

For the benefit of the reader, we recall the main premises of the $\mathbf{k} \cdot \mathbf{p}$ approximation. Although a number of methodologies quoted above (such as tight-binding and pseudo-potential) can provide us with the global dispersion relationships over the entire Brillouin zone for the bulk material, to know the main electronic characteristics of the semiconductor, such as wave functions, we need only the dispersion relationship over a small wave vector \mathbf{k} around the band extrema [24]. Indeed, it is well known that most processes in semiconductors take place near the top of the valence band and at the bottom of the conduction band [25]. The wave functions, characterizing wave propagation in the box volume $\Omega = \{(x, y, z) : 0 \leq x \leq L_x, 0 \leq y \leq L_y, 0 \leq z \leq L_z, \}$, are assumed to be in the form

$$\begin{aligned} \Phi_{lmn}(\mathbf{r}) &= (L_x L_y L_z)^{-1/2} \exp[i(k_x x + k_y y + k_z z)] = \\ &= (L_x L_y L_z)^{-1/2} \exp(i\mathbf{k} \cdot \mathbf{r}), \end{aligned} \quad (6)$$

where the allowed values of \mathbf{k}

$$\mathbf{k} = (2\pi l/L_x, 2\pi m/L_y, 2\pi n/L_z), \quad l, m, n = 0, \pm 1, \pm 2, \dots \quad (7)$$

form a 3D \mathbf{k} space with the origin denoted as Γ point. Based on this assumption, the application of Bloch's theorem in the context of semiconductor crystals leads to the following (Bloch) representation of the wave function in a crystal

$$\Phi_{n\mathbf{k}}(\mathbf{r}) = u_{n\mathbf{k}} \exp(i\mathbf{k} \cdot \mathbf{r}) \quad (8)$$

with $u_{n\mathbf{k}}$ being periodic. Since it is easier to find approximate solutions for the

function $u_{n\mathbf{k}}$ (assumed to be slowly varying over a small region of \mathbf{k} space) than for $\Phi_{n\mathbf{k}}$ [25], we attempt to write the Schrodinger equation in terms of $u_{n\mathbf{k}}$. In doing so, the derivatives of the momentum operator $\hat{\mathbf{p}} = -i\hbar\nabla$ acting on the plane waves are simplified to $\hbar\mathbf{k}$, leading to a simplification of the Schrodinger equation for the Bloch functions of the crystal, $\Phi_{n\mathbf{k}}$, where the terms depending on \mathbf{k} are treated as perturbations away from the solution at $\mathbf{k} = \mathbf{0}$. The presence of the operator $\mathbf{k} \cdot \hat{\mathbf{p}}$ in the resulting expression renders the name of the underlying local methodology. In this way, the standard parabolic approximations of the bands are refined locally in the $\mathbf{k} \cdot \mathbf{p}$ theory. This is important for the conduction band, but even more so for the valence band due to degenerating light and heavy holes at the Γ point.

It is worthwhile mentioning that another major reason for this particular choice of averaging lies with the fact that the $\mathbf{k} \cdot \mathbf{p}$ treats the bandstructure in a continuum-like manner, albeit allowing to incorporate many important effects acting at different scales which is very important for the problems like ours. This includes mechanical and electromechanical effects. As strain and piezoeffect are key contributors to changes in optoelectromechanical properties, the models described in the previous section must be incorporated in the bandstructure calculation. In order to do that, we first remind the reader that the accuracy of approximations based on the $\mathbf{k} \cdot \mathbf{p}$ theory depends on the functional space where the envelope function is considered. In fact, we put subbands within conduction and valence bands of the semiconductor material into correspondence to the basis functions that span such a space. The number of such functions varies in applications, but typically ranges from 1 to 8 to ensure computational feasibility of the problem. For WZ materials, 8 functions should usually be included due to spin-orbit, crystal-field splitting, as well as conduction/valence band mixing effects. This corresponds to 6 valence subbands and 2 conduction subbands that account for spin up and spin down situations. Given that the Hamiltonian in the $\mathbf{k} \cdot \mathbf{p}$ theory can be represented as

$$H = -\frac{\hbar^2}{2m_0} \nabla_i \mathcal{H}_{ij}^{(m,n)}(\mathbf{r}) \nabla_j, \quad (9)$$

the problem at hand can be formulated as an eigenvalue partial differential equation problem

$$H\Psi = E\Psi. \quad (10)$$

The standard Kohn-Luttinger representation of the Hamiltonian in the form of (9) is well documented in the literature and we refer the reader interested in details to books by G. Bastard and J. Singh, e.g. [24,26]. The problem (10) should be solved with respect to eigenpair (Ψ, E) , where E is the electron/hole

energy and Ψ is the wave vector with dimensionality of the functional space chosen. For example, in the situation discussed above we have

$$\Psi = (\psi_S^\uparrow, \psi_X^\uparrow, \psi_Y^\uparrow, \psi_Z^\uparrow, \psi_S^\downarrow, \psi_S^\downarrow, \psi_S^\downarrow, \psi_S^\downarrow)^T, \quad (11)$$

where the subindex S denotes the wave function component of the conduction band and $\psi_X^\uparrow \equiv (|X\rangle|\uparrow\rangle)$ is the wave function component that corresponds to the X Bloch function of the valence band when the spin function of the missing electron is up. In the Hamiltonian representation (9) \mathcal{H} is the energy functional, defined either by the standard Kohn-Luttinger Hamiltonian (as mentioned above) or by the Burt-Foreman modification [23]. It represents the kinetic energy plus a nonuniform potential field V and other effects contributing to the total potential energy of the system, as specified further in Section 4. Other notations are standard: \hbar is the Planck constant, m_0 is the free electron mass, $\mathbf{r} = (x_1 \equiv x, x_2 \equiv y, x_3 \equiv z)$, while the superindices (m, n) are used to denote the basis of the space for the wave function, which in the case discussed above (6 valence and 2 conduction subbands) would lead to an 8X8 Hamiltonian.

Four equations (3) of coupled electromechanics and the eigenvalue PDE problem (10) constitute a coupled Schrodinger-Poisson model that provides a general framework for incorporating nonlinear effects. Similar to the top-down approach, where coupling procedures are well established, in the bottom-up approach applied here the coupling between Schrodinger and Poisson equations is essential, in particular at the level of quantum device modelling.

5 Coupling strain with bandstructure calculations in the variational formulation

Since the fundamental work [15], strain effects firmly took their place in the models for bandstructure calculations of semiconductor structures. Many important examples of such calculations based on strained Rasba-Sheka-Pikus Hamiltonian have recently been provided in the context of low-dimensional semiconductor nanostructures, including quantum dots (e.g., [4]). However, all current models we are aware of have been based on linear theories. The first question to ask is whether material nonlinearities, expressed by stress-strain relationships, may become important for such calculations. The usual argument for using the linear stress-strain relationships in this field of applications is based on the fact that strain is indeed of order of magnitudes smaller of the elastic limits. Although this argument may fail at the device level modelling, it remains valid for the structures of interest in the present paper. At a more fundamental level, however, elastic and dielectric coeffi-

cients may become nonlinear due to geometry of the structure which will lead to nonlinear stress-strain relationships. To address this issue rigorously, one has to look critically at the standard Keating model where the parameters of the model are unit-cell dimension dependent. In the general case, we may need to account for many body interactions of higher order to reflect asymmetry of the interatomic potential. This issue is outside of the scope of the present paper. Instead, we will focus on a consequence of this issue that leads to geometric nonlinearities. Indeed, one of the major drawbacks of the current models for bandstructure calculations is that they are not able to resolve adequately strain nonhomogeneities due to the application of the original representation of [15] based the infinitesimal theory with Cauchy relationships between strain and displacements. As we demonstrate in the next section, this approximation is inadequate when we have to deal with geometric irregularities of low-dimensional semiconductor structures. In the latter case, by using the variation of deformation $\delta\varepsilon_{ij}$ which is induced by the variation in displacements δu_i , we describe the new position $\xi_i = x_i + u_i$ of the material particle (with initial coordinates x_i) after deformation. This leads naturally to the formulation of the problem where the general nonlinear Green-Lagrange relationship for strain can be accounted for. As we pointed out, the variational formulation of the problem at hand has been used before in the context of finite element implementations (e.g., [3,17,20]). Two new features that have been developed in this paper include (a) consistent coupled treatment of the piezoelectric effect and (b) the ability to incorporate geometric nonlinearities into the model. As we demonstrate in the next section, the influence of these features on the bandstructure calculations, and therefore optoelectromechanical properties of the modelled structures, could be substantial.

The case of weakly coupled piezoelectricity was analyzed previously in [18] where convergence results in Sobolev classes of generalized solutions were established. Indeed, in some special cases, in particular for simple boundary conditions, the problem can be addressed semi-analytically. In the context of quantum dots, this has been done in [6] by using Green's function approach. Strongly coupled problems of piezoelectricity have been analyzed previously from variational scheme perspectives in [16]. In the latter case, the steady-state formulation given by (3) should be understood in a variational sense as:

$$\int_{\tilde{V}} \left[-\sigma^T(\delta\varepsilon_L + \delta\varepsilon_N) + D\delta E \right] dv = 0, \quad (12)$$

where both piezoelectric stress and the nonlinear part of strain are taken into account via constitutive relationships with the total variation of deformation given by its linear and nonlinear parts $\delta\varepsilon = \delta\varepsilon_L + \delta\varepsilon_N$.

The above problem is coupled to the eigenvalue PDE problem, also understood

in a weak sense. That is we seek the solution to the following problem

$$\Phi(\Psi) \rightarrow \min, \quad \Psi \equiv -\frac{\hbar^2}{2m_0} \int_{\tilde{V}} (\nabla \Psi)^T \mathcal{H}^{(m,n)} \nabla \Psi dv - E \int_{\tilde{V}} \Psi^T \Psi dv, \quad (13)$$

where the Hamiltonian is given by (9). As usual in the $\mathbf{k} \cdot \mathbf{p}$ theory, formal representation can be reduced to the sum of constant and \mathbf{k} -dependent energies ($H = \bar{H} + V$):

$$\bar{H} = H_0 + \sum_{i=1}^3 H_i, \quad (14)$$

where H_0 , derived from the standard Kane Hamiltonian at $\mathbf{k} = \mathbf{0}$ (e.g., [24]), accounts for the spin-splitting effects; H_1 is the contribution due to the kinetic part of the microscopic Hamiltonian unit cell averaged by the respective Bloch functions, S, X, Y, or Z; H_2 is the strain-dependent part of the Hamiltonian, and H_3 is the energy of unstrained conduction/valence band edges.

In what follows we consider an example of modelling nanostructures based on the model described above. The main emphasis is given to a pyramidal quantum dot residing on a wetting layer. In [8] it was demonstrated that the electronic states in the wetting layer may influence electronic states in the dot and vice versa and, hence, the thin layer on which the quantum dot resides cannot be excluded from the computational domain as it is often done in the literature. This brings additional difficulties in the computational implementation of this multiscale problem.

6 Computational experiments on quantum dot nanostructures

Our representative example in this section concerns InAs/GaAs quantum dot structures of pyramidal shape. Such self-assembled structures are grown experimentally via Stranski-Krastanov methodology and have been studied before with simplified models of linear elasticity (e.g., [1,5]). As we have already mentioned, the present study has a number of new features. Firstly, we take the full electromechanical coupling as well as the wetting layer into account. Secondly, we analyze the influence of nonlinear strain components in modelling such quantum dot structures.

All our computational examples below are for the quantum dot structure presented in Fig. 1 where geometric dimensions are also given. Pyramidal shapes of quantum dot structures, such as the one we analyze, have been confirmed by

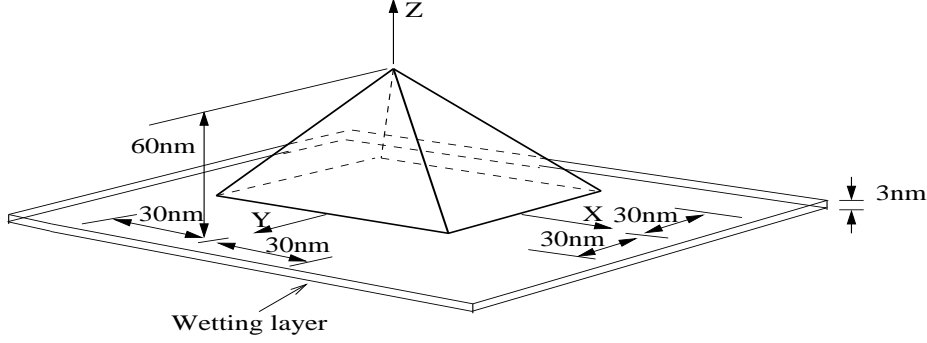


Fig. 1. Geometric dimensions of the representative pyramidal quantum dot.

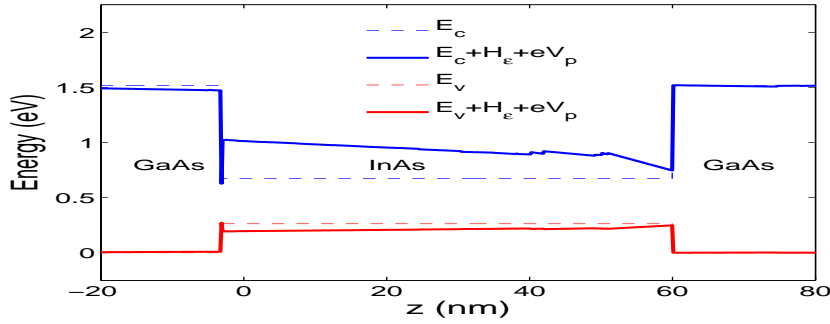


Fig. 2. Energy levels of the conduction and valence bands under the linear strain approximation.

experimental techniques, including high resolution electron microscopy. The entire structure, consisting of the InAs dot sitting on the wetting layer, is embedded in a (spherical) GaAs matrix. In such semiconductor materials one expects changes in the optoelectromechanical properties due to strain effects. However, up until now, such changes have been quantified with linear theories only. Hence, as the first step, in Fig. 2 we present energy levels for both conduction and valence bands by using the conventional methodology based on the linear approximation. This result is given at the center of the dot ($x = 0, y = 0$) along vertical z -axis.

A straightforward generalization of the linear theory in our context is to account for the large deformation gradient ∇u_3 . This gradient is responsible for the dominant nonlinear strain effect due to the lattice mismatch in the growth direction. While in the x and y directions the strain components will be identical in this case to the von Karman type model, in the z -direction they differ. As all the shear strain components are assumed in this case [Case I] to be linear, the Green-Lagrange strain components in this model take the form:

$$\varepsilon_{xx} = \frac{\partial u_1}{\partial x} + \frac{1}{2} \left(\frac{\partial u_3}{\partial x} \right)^2, \quad \varepsilon_{yy} = \frac{\partial u_2}{\partial y} + \frac{1}{2} \left(\frac{\partial u_3}{\partial y} \right)^2,$$

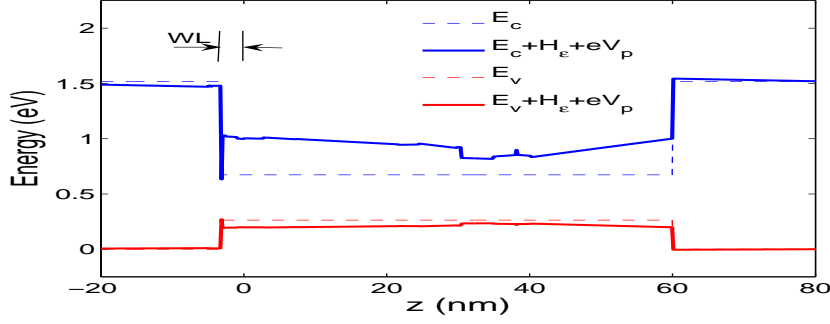


Fig. 3. Energy levels of the conduction and valence bands accounting for the large deformation gradient in the growth direction.

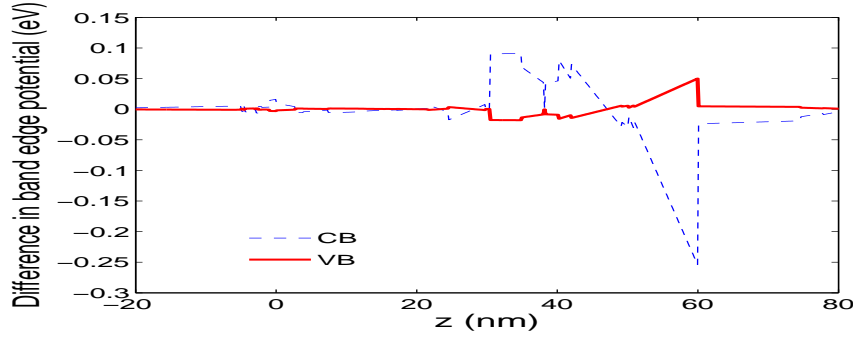


Fig. 4. Quantifying nonlinear contributions in the band edge potentials, accounting the large deformation gradient in the growth direction.

$$\varepsilon_{zz} = \frac{\partial u_3}{\partial z} + \frac{1}{2} \left(\frac{\partial u_3}{\partial z} \right)^2. \quad (15)$$

In this case, closer to the base of the dot, the behaviour of the energy levels are the same as in the linear case. However, the situation changes at the tip of the dot as can be seen from Fig. 3. As before, the result is presented at the center of the dot ($x = 0, y = 0$) along vertical z -axis.

Next, we have analyzed and quantified the difference between this nonlinear case and the linear case, conventionally used in these calculations. In Fig. 4 we present the difference in the band edge potential for the conduction and valence bands. This result demonstrates that nonlinear strain contributions could be substantial in calculating energy levels, and hence in predicting optoelectronic properties of nanostructures. In our case these contributions are particular pronounced for the conduction band.

The comparisons indicate the maximum deviation from the linear theory near the top vertex of the pyramid of 60nm high, not at the wetting layer. Indeed, due to the lattice mismatch at the wetting layer and pyramid interface, components like $(\partial u_1 / \partial x)^2$ and $(\partial u_2 / \partial y)^2$ will become important, rather than



Fig. 5. Biaxial and isotropic strains at $y=0$.



Fig. 6. Biaxial and isotropic strains at $z=1.5\text{nm}$

$(\partial u_3/\partial x)^2$ or $(\partial u_3/\partial y)^2$ which are due mainly to the Poisson effect in this problem.

These differences between the results produced with the linear and nonlinear models are hard to quantify without the band edge potentials, as presented above. Indeed, we have calculated a number of other characteristics, including biaxial strain

$$\varepsilon_b = (\varepsilon_{11} - \varepsilon_{22})^2 + (\varepsilon_{22} - \varepsilon_{33})^2 + (\varepsilon_{33} - \varepsilon_{11})^2 \quad (16)$$

and isotropic strain

$$\varepsilon_i = \varepsilon_{11} + \varepsilon_{22} + \varepsilon_{33}. \quad (17)$$

In Fig. 5 we present biaxial and isotropic strains in the $y=0$ plane.

These characteristics are shown also just above the wetting layer, at $z=1.5\text{nm}$, in Fig. 6. In both of the above situations we chose to present the results of calculations produced with the conventional methodology, while noting that calculations obtained with nonlinear contributions look very similar.

In Fig. 7 we present the distribution of the piezoelectric potential in the quantum dot under consideration (as well as its projection from the top). Recall that results with uncoupled or semi-coupled models usually demonstrate max-



Fig. 7. Distribution of the piezoelectric potential in the quantum dot.

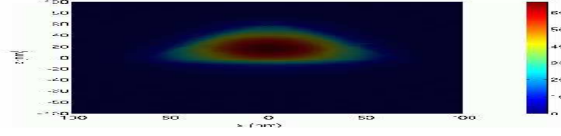


Fig. 8. Ground state of the quantum dot nanostructure.

ima of the piezopotential outside of ZB quantum dot structures only, in particular when the dot is truncated. This is, of course, not the case for the coupled model applied in the current situation. The local extrema of the piezoelectric potential near the QD top can be well reproduced, as demonstrated by Fig. 7. As expected, the distribution is symmetric at the bottom and at the top of the pyramid. We note also that predicting optoelectromechanical properties of hexagonal (WZ) materials usually requires to account for an additional effect of spontaneous polarization, typically negligible in ZB materials. As described in Section 2, our model is capable of dealing with both types of the materials.

Next, we have calculated eigenstates of the structure. The ground state, presented in Fig. 8, has been calculated accounting for strain and piezoelectric effects. As seen from the figure, the state is fully confined.

In Fig. 9 the next four eigenstates of the nanostructure are presented. As confinement visualization looks similar for both linear and nonlinear cases, we shall provide calculated numerical values that demonstrate the influence of piezoelectric effect as well as nonlinear contributions on electronic states.

Before doing that, we recall that the only nonlinear model we considered so far was the model accounting for the large deformation gradient in the growth direction. We have also analyzed the case where we account for the large deformation gradients ∇u_1 and ∇u_2 , responsible for the dominant nonlinear

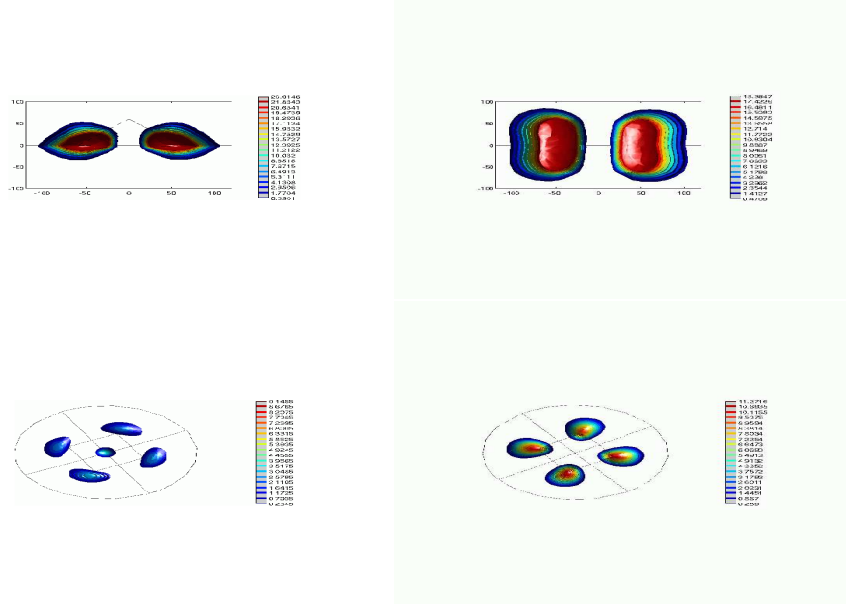


Fig. 9. Electronic confinement in the quantum dot nanostructure: the 2nd, 3rd, 4th, and 5th eigenstates.

strain effects due to the lattice mismatch in the $x - y$ plane, normal to the growth direction. In this case [Case II] the Green-Lagrange strain components are:

$$\begin{aligned}\varepsilon_{xx} &= \frac{\partial u_1}{\partial x} + \frac{1}{2} \left(\frac{\partial u_1}{\partial x} \right)^2 + \frac{1}{2} \left(\frac{\partial u_2}{\partial x} \right)^2, \\ \varepsilon_{yy} &= \frac{\partial u_2}{\partial y} + \frac{1}{2} \left(\frac{\partial u_1}{\partial y} \right)^2 + \frac{1}{2} \left(\frac{\partial u_2}{\partial y} \right)^2, \\ \varepsilon_{zz} &= \frac{\partial u_3}{\partial z} + \frac{1}{2} \left(\frac{\partial u_1}{\partial z} \right)^2 + \frac{1}{2} \left(\frac{\partial u_2}{\partial z} \right)^2,\end{aligned}\tag{18}$$

while all the shear strain components remain linear. As expected in this case, the results show nonlinear effect contributions due to the nonlinear relaxation of the interfacial strain between the InAs wetting layer and the GaAs matrix.

Next, we implemented the full nonlinear strain model [Case III] in the developed finite element code, based on the general Green-Lagrange strain

$$\boldsymbol{\varepsilon} = \frac{1}{2}(\mathbf{F}^T \mathbf{F} - \mathbf{I}),\tag{19}$$

where \mathbf{F} is the deformation gradient and \mathbf{I} is the identity matrix. In Figs. 10–12 the results are presented along the z -axis ($y=0$) for the three cases: $x=0$,

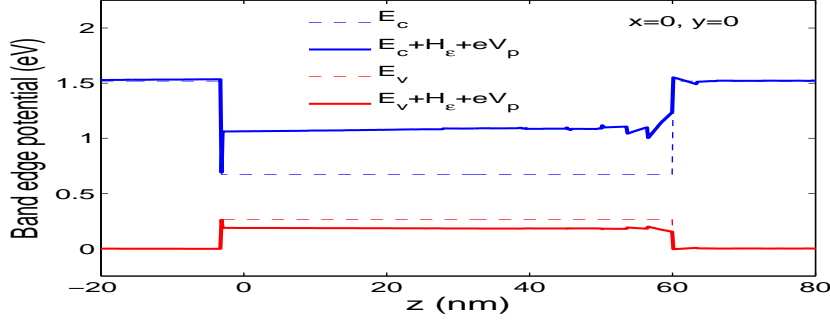


Fig. 10. The band edge potential with the full nonlinear strain model ($x=0, y=0$).

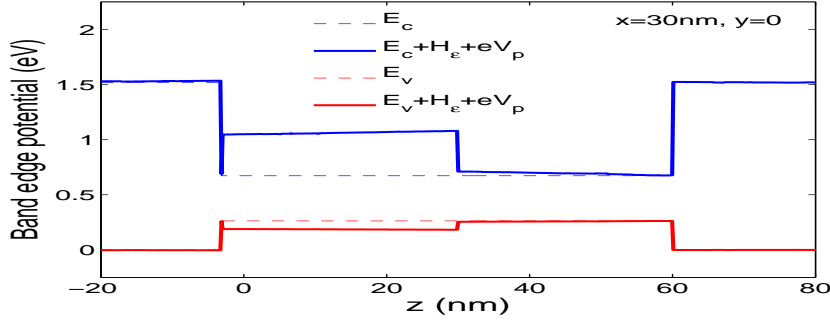


Fig. 11. The band edge potential with the full nonlinear strain model ($x=30, y=0$).

30, and 60 nm, respectively. Although differences with calculations obtained with the linear model are clearly observed, we quantify them in Table 1. The first column in the table is the number of the corresponding eigenstate. The second column gives eigenstates obtained with the linear theory, accounting for strain only; the third column gives eigenstates obtained with the linear theory, accounting for strain and piezo effects. The remaining columns give the results obtained with the nonlinear models based on Cases I, II, and III, respectively, as described above. All values are given in eV.

In all finite element computations reported here we applied tetrahedral elements with quadratic Lagrangian interpolation function. The global convergence was analyzed by refining the finite element mesh and ensuring that the difference between the last two subsequent refinements is negligible in L_2 . For the solution of the discretized equations we used GMRES with incomplete Cholesky factorization. The maximum number of iteration was set to 500 and the L_2 error tolerance was set as 1×10^{-6} . The pyramid was embedded into a sphere. The loading conditions were simulated by subjecting the outer surface of the sphere to Dirichlet boundary conditions in displacement. The pyramid structure was allowed to equilibrate under the combined effect of lattice misfit induced strain and piezoelectric polarization.

Finally, we calculate the bandstructure with our finite element method code and compare the band edge potential due to the above three nonlinear strain

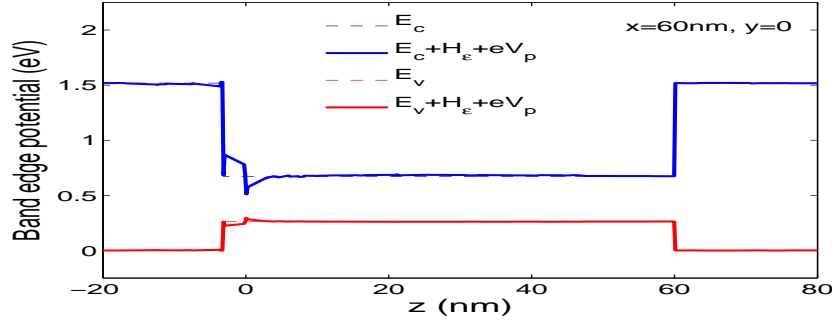


Fig. 12. The band edge potential with the full nonlinear strain model ($x=60$, $y=0$).

Eigenstate #	Lin/strain	Lin/strain+piezo	Case I	Case II	Case III
1	0.7122	0.6968	0.6811	0.6913	0.6767
2	0.8345	0.8084	0.8008	0.8070	0.7994
3	0.8404	0.8115	0.8046	0.8095	0.8027
4	0.8511	0.8272	0.8248	0.8267	0.8244
5	0.8658	0.8350	0.8321	0.8345	0.8316

Table 1

The influence of strain, piezoeffects, and nonlinear contributions on eigenstates of the structure.

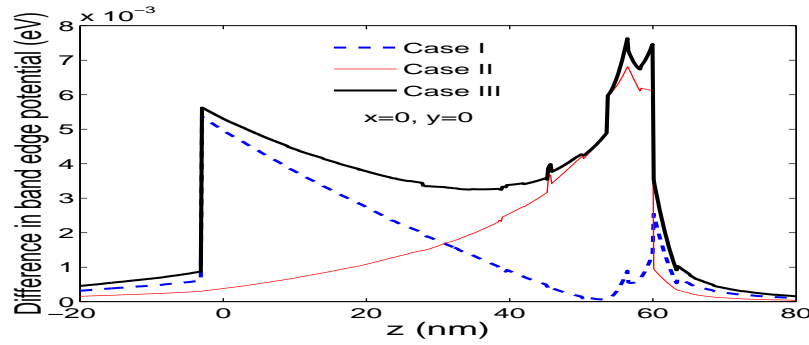


Fig. 13. Quantifying the difference between linear and nonlinear models in the presence of piezoeffect ($x=0$, $y=0$).

models in the presence of piezoelectricity. The difference for each of these three cases of band edge potentials with respect to that of the linear case is computed and plotted along the z -axis for (a) $x = 0, y = 0$, (b) $x = 30\text{nm}, y = 0$, and (c) $x = 60\text{nm}, y = 0$ in Figs. 13–15, respectively. It is clear from the plots that the fully nonlinear strain model (Case III) captures the large inhomogeneous strain-induced band edge potential as a cumulative effect of the potentials for Cases I and II. The band edge potentials along the presented $[001]$ direction (z -axis) for each of these three cases have been computed with the fully coupled model.

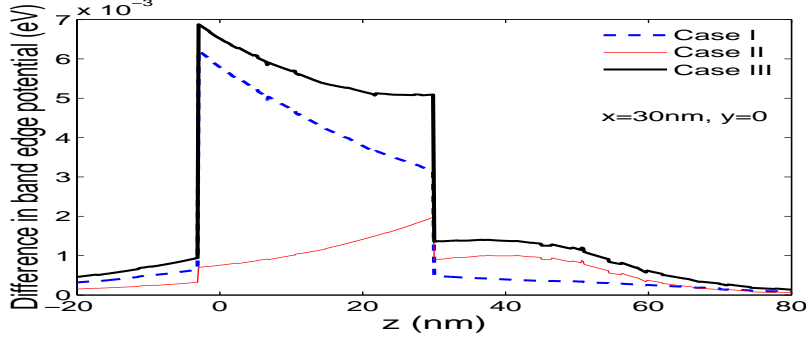


Fig. 14. Quantifying the difference between linear and nonlinear models in the presence of piezoeffect ($x=30$, $y=0$).

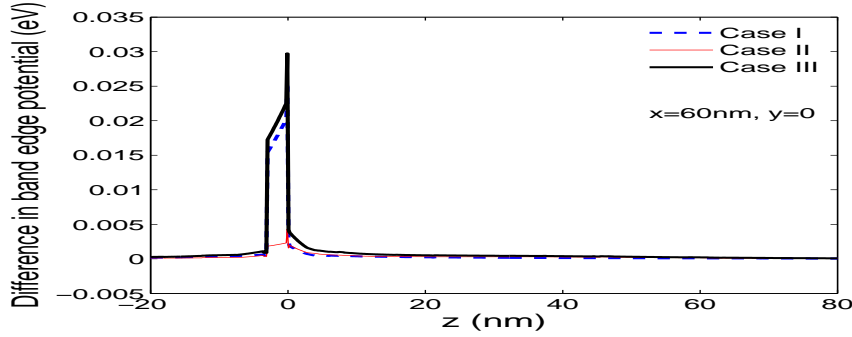


Fig. 15. Quantifying the difference between linear and nonlinear models in the presence of piezoeffect ($x=60$, $y=0$).

7 Conclusions

In this contribution, we analyzed two fundamental approaches in bridging the scales in mathematical models for the description of optoelectromechanical properties of nanostructures. We demonstrated that the conventional application of linear models to the analysis of properties of nanostructures in bandstructure engineering could be inadequate. By accounting consistently for the piezoelectric effect, we considered three nonlinear strain models and analyzed contributions of quadratic nonlinear terms induced by the deformation gradient in the growth direction, as well as in the plane normal to that direction. The core of our model was based on the Shrodinger-Poisson system which was presented in the variational form and implemented with finite element methodology. In this framework, we presented also the full nonlinear strain model and quantify the differences between the conventional linear and developed here nonlinear models for bandstructure calculations. Generalizations of the existing models and the examples provided for quantum dot nanostructures emphasized the importance of coupled effects in predicting optoelectromechanical properties of such structures.

Acknowledgments

This work was supported by NSERC. The authors thank Profs M. Willatzen (Denmark), L.C. Lew Yan Voon (USA), and Dr B. Lassen (Sweden) for fruitful discussions on LDSN modelling issues and the anonymous referees for a number of useful suggestions incorporated in the final version of this paper.

References

- [1] Grundmann M, Stier O, Bimberg D. InAs/GaAs pyramidal quantum dots: strain distribution, optical phonons, and electronic structure. *Phys. Rev. B* 1995; 52(16): 11969.
- [2] Andreev AD, O'Reilly EP. Theory of the electronic structure of GaN/AlN hexagonal quantum dots. *Phys. Rev. B* 2000; 62(23): 15851–15870.
- [3] Johnson HT, Bose R. Nanoindentation effect on the optical properties of self-assembled quantum dots. *J. Mech. Phys. Solids*. 2003; 51: 2085–2104.
- [4] Fonoberov VA, Balandin AA. Excitonic properties of strained wurtzite and zincblende $GaN/Al_xGa_{1-x}N$ quantum dots. *J. Appl. Phys.* 2003; 94(11): 7178–7186.
- [5] Kuo MK, Lin TR, Hong KB et al. Two-step strain analysis of self-assembled InAs/GaAs quantum dots. *Semicond. Sci. Technol.* 2006; 21: 626–632.
- [6] Pan E. Elastic and piezoelectric fields around a quantum dot: fully coupled or semicoupled model? *J. Appl. Phys.* 2002; 91(6): 3785–3796.
- [7] Jogai B, Albrecht, JD, Pan E. Effect of electromechanical coupling on the strain in AlGaIn/GaN HFETs. *J. Appl. Phys.* 2003; 94: 3984–3989.
- [8] Melnik RVN, Willatzen M. Bandstructures of conical quantum dots with wetting layers. *Nanotechnology*. 2004; 15: 1–8.
- [9] Willatzen M., Melnik RVN, Galeriu C., and Lew Yan Voon LC. Quantum confinement phenomena in nanowire superlattice structures. *Mathematics and Computers in Simulation*. 2004; 65(4-5): 385–397.
- [10] Bass F.G. and Bulgakov A.A. *Kinetic and Electrodynamical Phenomena in Classical and Quantum Semiconductor Superlattices*. Nova Science Publisher. 1997.
- [11] Melnik RVN, He H. Relaxation-time approximations of quasi-hydrodynamic type in semiconductor device modelling. *Modelling and Simulation in Materials Science and Engineering*. 2000; 8(2): 133–149.
- [12] Melnik RVN, He H. Quasi-hydrodynamic modelling and computer simulation of coupled thermo-electrical processes in semiconductors. *Mathematics and Computers in Simulation*. 2000; 52(3-4): 273–287.

- [13] Rudan M, Gnani E, Reggiani S, Baccarani G. A coherent extension of the transport equations in semiconductors incorporating the quantum correction. *IEEE Transactions on Nanotechnology*. 2005; 4(5): 495-509.
- [14] Ipatova IP, Malyshkin VG, Shchukin VA. On spinoidal decomposition in elastically anisotropic epitaxial films of III-V semiconductor alloys. *J. Appl. Phys.* 1993; 74(12): 7198–7210.
- [15] Bir GL, Pikus GE. Symmetry and strain-induced effects in semiconductors. New York: Wiley, 1974.
- [16] Melnik RVN, Zotsenko KN. Mixed electrostatic waves and CFL stability conditions in computational piezoelectricity. *Appl. Numer.* 2004; 48(1): 41–62.
- [17] Melnik RVN, Zotsenko KN. Finite element analysis of coupled electronic states in quantum dot nanostructures. *Model. Simul. Mater. Sci. Eng.* 2004; 12(3): 465–477.
- [18] Melnik RVN, Melnik KN. A note on the class of weakly coupled problems of non-stationary piezoelectricity. *Commun. Numer. Meth. Engnr.* 1998; 14: 839–847.
- [19] Melnik RVN. Generalized solutions, discrete models and energy estimates for a 2D problem of coupled field theory. *Appl. Math. Comput.* 2000; 107: 27–55.
- [20] Voss H. Numerical calculation of the electronic structure for three-dimensional quantum dots. *Comp. Phys. Comm.* 2006; 174: 441–446.
- [21] Melnik RVN, He H. Modelling nonlocal processes in semiconductor devices with exponential difference schemes. *J. Eng. Math.* 2000; 38: 233–263.
- [22] Bourgade JP, Degond P, Mehats F, Ringhofer C. On quantum extensions to classical spherical harmonics expansion/Fokker-Planck models. *J. Math. Phys.* 2006; 47 (4): 043302.
- [23] Lassen B, Voon LCLY, Willatzen M, Melnik RVN. Exact envelope-function theory versus symmetrized Hamiltonian for quantum wires: a comparison. *Solid State Communications*. 2004; 132(3-4): 141–149.
- [24] Bastard G. Wave mechanics applied to semiconductor heterostructures. New York: Halsted Press (a division of John Wiley & Sons), 1988.
- [25] Davies JH. The physics of low-dimensional semiconductors. Cambridge: Cambridge University Press, 1998.
- [26] Singh J. Physics of semiconductors and their heterostructures. New York: McGraw-Hill, 1993.